Published in final edited form as:
Neurobiol Dis. 2012 January ; 45(1): 395–408. doi:10.1016/j.nbd.2011.08.029.

Core features of frontotemporal dementia recapitulated in progranulin knockout mice

N. Ghoshal[a], **J.T. Dearborn**[b], **D.F. Wozniak**[b], and **N.J. Cairns**[a,c]

[a]Department of Neurology, Washington University School of Medicine, St. Louis, MO 63110, USA

[b]Department of Psychiatry, Washington University School of Medicine, St. Louis, MO 63110, USA

[c]Department of Pathology & Immunology, Washington University School of Medicine, St. Louis, MO 63110, USA

Abstract

Frontotemporal dementia (FTD) is typified by behavioral and cognitive changes manifested as altered social comportment and impaired memory performance. To investigate the neurodegenerative consequences of progranulin gene (*GRN*) mutations, which cause an inherited form of FTD, we used previously generated progranulin knockout mice *(Grn-/-)*. Specifically, we characterized two cohorts of early and later middle-age wild type and knockout mice using a battery of tests to assess neurological integrity and behavioral phenotypes analogous to FTD. The *Grn*-/- mice exhibited reduced social engagement and learning and memory deficits. Immunohistochemical approaches were used to demonstrate the presence of lesions characteristic of frontotemporal lobar degeneration (FTLD) with *GRN* mutation including ubiquitination, microgliosis, and reactive astrocytosis, the pathological substrate of FTD. Importantly, *Grn*-/- mice also have decreased overall survival compared to *Grn*+/+ mice. These data suggest that the *Grn*-/- mouse reproduces some core features of FTD with respect to behavior, pathology, and survival. This murine model may serve as a valuable *in vivo* model of FTLD with *GRN* mutation through which molecular mechanisms underlying the disease can be further dissected.

Keywords

Frontotemporal lobar degeneration; frontotemporal dementia; knockout mouse; neurodegeneration; social behavior; memory; ubiquitin; progranulin

Introduction

Frontotemporal dementia (FTD) represents 5-20% of all dementia cases and is the second most frequent dementia in people under the age of 65 years (Neary et al., 1998).

Corresponding author: Nupur Ghoshal, MD, PhD, Charles F. and Joanne Knight Alzheimer's Disease Research Center, Department of Neurology, Washington University School of Medicine, 4488 Forest Park Avenue, Suite 101, St. Louis, MO 63108, Tel: 1-314-286-2683, Fax: 1-314-286-2448, ghoshaln@neuro.wustl.edu.

Author Disclosure Information: N. Ghoshal, has participated or is currently participating in clinical trials of antidementia drugs sponsored by: Bristol-Myers Squibb, Elan/Janssen, Eli Lilly, Novartis, Pfizer, and Wyeth; J.T. Dearborn, None; D.F. Wozniak, None; N.J. Cairns, None.

Frontotemporal lobar degeneration (FTLD), the pathology causing FTD, is heterogeneous. Three FTD phenotypes are recognized: behavioral variant FTD (bvFTD), primary progressive aphasia (PPA) and semantic dementia (SD); these are initially characterized by changes in behavior, personality, and language with dementia and parkinsonism appearing late in the disease (McKhann et al., 2001). Behavioral changes include altered social comportment, lack of motivation, withdrawal, and apathy. Memory deficits are manifested by impaired social learning and memory performance. Dominantly inherited FTD comprises 5-10% of all FTD cases, with mutations in the progranulin gene (*GRN*) accounting for 53% of familial FTD (http://www.molgen.ua.ac.be/FTDMutations). Mutations in the progranulin gene co-segregate with affected individuals in these kindreds and have also been identified in cases of sporadic FTD (Baker et al., 2006; Cruts et al., 2006; Gass et al., 2006; Mesulam et al., 2007; Mukherjee et al., 2006). The pathology of FTLD with *GRN* mutation is characterized by focal atrophy of the frontal and temporal lobes and the striatum is frequently affected. Microscopy reveals the signature lesions of all FTLD entities: neuronal loss, gliosis, and ubiquitin-immunoreactive neuronal inclusions in affected areas. The pathological protein of the ubiquitinated inclusions in FTLD with *GRN* mutation has been identified as the TAR DNA-binding protein of 43 kDa (TDP-43) and TDP-43-positive aggregates are found at four sites: neuronal cytoplasmic inclusions (NCI), neuronal intranuclear inclusions (NII), dystrophic neurites (DN), and glial cytoplasmic inclusions (GCI) that are negative for tau, α-synuclein, β-amyloid and FUS (Cairns et al., 2007; Mackenzie et al., 2010).

Progranulin is a 593 amino acid precursor protein, which is further processed to 6 kDa active peptides called granulins (Bateman and Bennett, 2009). In the periphery, intact progranulin is a secreted growth factor that causes tumorigenicity when overexpressed and impaired cell growth and proliferation when less abundant (Bateman and Bennett, 2009). Moreover, progranulin and the granulins appear to have opposing effects. Progranulin functions are trophic and anti-inflammatory, whereas the granulins exhibit pro-inflammatory activity (Bateman and Bennett, 2009). However, the physiologic function of progranulin in the CNS or the mechanism by which it leads to neurodegeneration remain open questions. Most progranulin mutations introduce a premature termination codon leading to nonsense-mediated decay with resultant absence of the mutant *GRN* transcript. This loss of functional *GRN* implicates a haploinsufficiency mechanism for neurodegeneration (Bateman and Bennett, 2009).

Since the discovery of progranulin mutations in 2006 (Baker et al., 2006; Behrens et al., 2007; Cruts et al., 2006; Gass et al., 2006; Mesulam et al., 2007; Mukherjee et al., 2006), there has been an interest in developing mouse models of progranulin deficiency with the expectation that aspects of the FTD phenotype will be exhibited by the mice. In 2007, the first *Grn* knockout mice were simply generated by homologous recombination (exons 2-13 removed) and were described by Kayasuga and colleagues (Kayasuga et al., 2007). These *Grn* knockout mice are born with an expected Mendelian distribution and appear to grow and develop normally. Young 7-11 week old *Grn* knockout males exhibited enhanced aggressiveness and anxiety (Chiba et al., 2009; Kayasuga et al., 2007). In the current study, we used these mice to investigate the neurodegenerative consequences of *GRN* mutations. Specifically, we characterized two cohorts of early and later middle-age wild type (*Grn*+/+) and knockout (*Grn*-/-) mice using a battery of tests to assess neurological integrity and behavioral phenotypes analogous to FTD. Furthermore, immunohistochemical approaches were used to ascertain the presence of pathologic lesions characteristic of FTLD. Data presented here suggest that the *Grn*-/- mouse reproduces some analogous aspects of the FTD behavioral and FTLD pathological phenotypes.

Materials and methods

Animals

Progranulin knockout mice (*Grn*-/-) were previously generated by insertion of the neomycin resistance gene into mouse *Grn* gene replacing exons 2-13 by homologous recombination (Kayasuga et al., 2007). The colony was expanded and maintained on a C57BL/6 background (Jackson Laboratory, Bar Harbor, ME). *Grn*-/- and *Grn*+/+ animals were obtained by mating heterozygote animals. Genomic DNA was obtained by tail biopsy at postnatal day 5 and genotyping was confirmed by polymerase chain reaction assay for both the WT (wild type) and KO (knockout) alleles. WT status was determined using the following primer set: 5′-TGCAGATGGGAAATCCTGCTTCCAGATGTC-3′ and 5′-TCCCCACGAACCATCAACCATAATGCAGCA-3′. KO status was determined using the following primer set: 5′-CCAATATGGGATCGGCCATTGAAC-3′ and 5′-CGCTCGATGCGATGTTTCGCTTGG-3′. Mice were housed and cared for in animal facilities administered through the Washington University Division of Comparative Medicine. All animal procedures were performed according to protocols approved by the Washington University Animal Studies Committee.

Experimental design of behavioral studies

The behavioral studies were conducted in two cohorts of mice (Table 1). A 1-h locomotor activity/exploratory behavior test and a battery of sensorimotor measures were administered to the *Grn*-/- (n=12; 8M, 4F) and *Grn*+/+ (n=8; 7M, 1F) mice in the first cohort when they were 9-12 months of age. Cognitive testing was conducted at an older age (i.e., 13-16 months; Table 1) so that the mice would be roughly comparable in physiology to middle-aged and older humans (Turnbull et al., 2003). Because of the original report of enhanced aggression in young (7-11 week old) *Grn* -/- mice (Kayasuga et al., 2007), both groups of mice were assessed for their reactivity to handling three days after completing the sensorimotor battery, and twelve days after that, the resident intruder test was conducted. After an intervening period of four months when the mice were 13-16 months of age, they were tested on the Morris water maze to study their spatial learning and memory capabilities.

To provide enhanced statistical power for evaluating water maze performance and to gain a more even distribution of gender across genotypes, a second independent cohort of mice [*Grn*-/-: n=14; 4M,10F and *Grn*+/+: n=12; 4M, 8F] was tested on the water maze task at the same age (13-16 months) and the data from the two cohorts were combined for statistical analyses involving traditional water maze variables (Table 1). An olfactory preference test, the 1-h locomotor activity test, and battery of sensorimotor measures were also administered to this second cohort (Table 1). Mice from the second cohort were also tested on a learning set protocol in the water maze approximately 10 weeks after completion of the traditional water maze testing when they were 16-19 months old (Table 1).

1-hr locomotor activity/exploratory behavior test and sensorimotor battery

Locomotor activity and exploratory behaviors were evaluated in all mice over a 1-h period using computerized photobeam instrumentation as previously described (Wozniak et al., 2004). General activity variables (total ambulations, rearings) along with measures of emotionality, including time spent, distance traveled and entries made in a 33 × 11 cm central zone, as well as distance traveled in 5.5 cm wide peripheral zone around the edge of the chamber were analyzed. All mice were also evaluated on a battery of sensorimotor tests (walking initiation, ledge, platform, 90° inclined screen, inverted screen, and pole) designed to assess balance, strength, and coordination, as previously described (Wang et al., 2002; Wozniak et al., 2004).

Reactivity to handling

Three days after completing testing on the battery of sensorimotor measures, the mice from cohort 1 were assessed on a reactivity to handling test using our previously described procedures (Gallitano-Mendel et al., 2007). A five-point scale was used to rate a mouse during each of 3 sessions with a score of "1" indicating hyporeactivity to handling (little or no resistance to being captured, picked up, and handled) at one end of the scale, and a score of "5" indicating hyper-reactivity to handling (extreme resistance to capture as well as frequent jumping, biting and escape-related behaviors) at the other end (see Gallitano-Mendel et al., 2007 for greater details). Means were computed from the ratings of the three "blinded" evaluators such that each mouse was assigned a single score for each of the three sessions.

Resident-intruder

The resident-intruder test was administered to all male mice in the first cohort (N = 15) using a protocol similar to our previously published methods (Gallitano-Mendel et al., 2008). Males were individually housed for 4 weeks prior to testing. During testing, an unfamiliar male "intruder" was placed in the home cage of a subject mouse. Three 10-minute sessions, (one session on each of three consecutive days), were videotaped and agonistic interactions and other behaviors were scored by a rater who was "blinded" to the genotype of each mouse. An aggression index score was calculated for each mouse on each test day, which was composed of the summated durations of fighting and biting. Measures such as pawing, following, and time spent alone were also quantified.

Holeboard olfactory preference

Grn-/- and *Grn*+/+ mice in the second cohort (N = 23) were evaluated for possible differences in olfactory preference using our own modified version of a previously published procedure (Moy et al., 2008). Our protocol involves the use of a computerized holeboard apparatus (16 in × 16 in), containing 4 corner and 4 side holes, with a side hole being equidistant between the corner holes (Learning Holeboard; MotorMonitor, Kinder Scientific, LLC, Poway, CA). Pairs of photocells were contained within each hole (27 mm in diameter) and were used to quantify the frequency and duration of pokes. Specifically, a mouse was required to place its head into a hole at a depth of at least 35 mm and break a photobeam in order for the response to be registered as a hole poke. Odorants were placed at the bottom of two opposing corner holes although access to the odorants was blocked. Mice were administered a 1-h trial on each of four test days. The first day involved habituation to the apparatus without the presence of experimental odors. On the second day, fresh corncob bedding was placed in 2 corner holes while all other holes remained empty. This odorant was familiar in that it was used in the home cages of the mice. On the third day, a novel odorant (filter paper impregnated with 2 ml of coconut extract) was placed in 2 of the corner holes. After testing on the third day, mice were exposed to a small amount of fruit-flavored cereal in their home cages. The following day, food was removed from the home cages and after overnight food restriction, a final 1-h trial was administered which involved placing the fruit-flavored cereal in the bottom of 2 corner holes. Holes containing odorants were counterbalanced between and within groups. Dependent variables included total numbers of hole pokes and average number of hole pokes per hole type (odorant vs empty). The latter variable involved dividing the total number of pokes in each type of hole by the number of holes of that type, i.e., 2 odorant or 6 empty holes.

Morris water navigation

Spatial learning and memory were evaluated in the Morris water maze using a computerized tracking system (PolyTrack, San Diego Instruments, San Diego, CA) utilizing procedures

similar to those previously described (Wozniak et al., 2004; Wozniak et al., 2007). The protocol included conducting cued (visible platform, variable location), place (submerged, hidden platform, constant location), and probe (platform removed) trials where escape path length and latency, and swimming speeds were calculated for the cued and place trials. [See Supplemental Information for additional details.]

Learning set water maze

Approximately 10 weeks after completion of traditional water maze testing, mice in the second cohort (N=23) were tested on a learning set protocol in the water maze using a procedure similar to one we have used in rats (Hartman et al., 2005). Briefly, mice were trained using methods resembling those utilized during the place condition except that a new platform location was used on each of five consecutive days and no probe trial was administered. On each day, four trials were conducted [60-s maximum; 30-s inter-trial interval (ITI), (15 s on the platform and 30 s in a holding cage)] which were split into blocks of two, with each block being separated by approximately 1 h where the platform location and sequence of starting points were pseudo-randomly varied across test days. Group performances were compared on trial 2 since it represents a measure of short-term working memory where the mouse must recall the platform location on the immediately preceding trial rather than what it had learned previously in the water maze. General acquisition performance was also evaluated by quantifying the daily improvement from trial 1 to trial 4 within each group.

Tissue processing

Animals from different age groups ranging from 10 weeks to 24 months were deeply anesthetized by intraperitoneal injection of ketamine/xylazine cocktail and tissues were fixed by intracardiac perfusion with phosphate-buffered saline (PBS) followed by 4% paraformaldehyde. Brains were harvested and post fixed in 4% paraformaldehyde. After paraffin embedding, coronal sections were cut at 6μm.

Histology

To determine the anatomical distribution of pathology, coronal slices were taken at multiple levels to include: olfactory bulb, cerebral cortex, striatum, hippocampus, dentate gyrus, thalamus, hypothalamus, midbrain, pons, medulla oblongata, and cerebellum. Six **u**m sections were stained with hematoxylin and eosin (H&E) and cresyl violet. Immunohistochemistry was performed on deparaffinized and rehydrated sections. For β-amyloid, phospho-TDP43, phospho-α-synuclein, and casein kinase-1 immunohistochemistry, sections were pretreated with formic acid (98%) to enhance antigen retrieval. Sections were incubated with the following primary antibodies: sheep anti-mouse progranulin (1:600; R&D, Minneapolis, MN), mouse monoclonal phospho-TDP-43 (1:40,000; CosmoBio, Carlsbad, CA), rabbit polyclonal anti-ubiquitin (1:4,000; DAKO, Carpinteria, CA), rabbit polyclonal anti-GFAP (1:1,000; DAKO, Carpinteria, CA), rabbit polyclonal IBA-1 (1:3,000; Wako, Richmond, VA), mouse monoclonal anti-β-amyloid 10D5 (1:100,000; Eli Lilly, Indianapolis, IN), mouse monoclonal PHF-1 (1:500; a gift from Dr. Peter Davies, Albert Einstein College of Medicine, New York, NY), mouse monoclonal phospho-α-synuclein (1:10,000; Wako, Richmond, VA), mouse monoclonal CK-1 (1:250; Chemicon, Temecula, CA), rabbit polyclonal anti-synaptophysin (1:1,000; Abcam, Cambridge, MA), and mouse monoclonal NeuN (1:1,000; Chemicon, Temecula, CA). Species-specific biotinylated secondary antibodies were applied followed by avidin-horseradish peroxidase, and the chromogenic substrate diaminobenzidine tetrahydrochloride (DAB; Vector Laboratories, Burlingame, CA) was used for detection of horseradish peroxidase. To ensure even staining between sections, all sections were stained as a batch.

Sections were counterstained with hematoxylin. Additional sections were set aside for quantitative densitometry and were not counterstained.

Estimation of neuron numbers

Stereological counts of NeuN-positive neurons were undertaken in 20μm sections adjacent to those used for quantitative immunohistochemistry (see below). Three sites were investigated: the CA1 subfield of the hippocampus, the cortex extending from the retrospenial granular cortex to the secondary somatosensory cortex, and the dorsal thalamus (including the lateral and medial dorsal thalamus) at Bregma ~ -1.6 (Paxinos and Franklin, 2001). To make unbiased estimates of neuron numbers in the three brain regions, the optical fractionator probe was used, as implemented by the Stereo Investigator software package (MicroBrightField, Williston, VT) and a Nikon E800 microscope with motorized stage in three dimensions. Briefly, a three-dimensional counting probe (x, y, and z dimensions of 50 × 50 × 10 μm, respectively) was applied to a systematic random sample of sites at each of the three sites. The outline of the area of interest was outlined using a 4x objective (cortex: ~4mm^2; thalamus: ~2mm^2; and CA1 subfield: ~0.2mm^2) and the neuron count was determined using a 100× oil immersion lens with a high numerical aperture (NA = 1.40) which allows for the focusing of a thin focal plane inside a thick section. Each NeuN-positive neuron with a visible nucleus and nucleolus was counted as the experimenter focused down through 10 μm of tissue. Variations in section thickness caused by shrinkage during tissue processing restricted the guard border to 1 to 4 μm. Pilot studies determined the variables of Stereo Investigator, including the size of the counting brick and sampling grid, to yield results with a coefficient of error (m = 0) (Gundersen and Jensen, 1987) for the population estimate of 0.05 to 0.1. The volume of the sampling area was estimated using the Cavalieri estimator (Fabricius et al., 2008) and together with the estimate of the total number of neurons obtained from the optical fractionator, an estimate of the neuronal density, N_v (cells/mm^3) was obtained.

Quantitative immunohistochemistry of DAB-stained sections

As we used several antibodies with optically continuous staining characteristics (variable grey scale intensities) and heterogeneous morphological features, we employed computerized quantitative densitometric techniques as previously described (Ghoshal et al., 2001; Ghoshal et al., 2002). Quantitation of immunoreactive lesions on non-counterstained sections was undertaken by a single observer (NG) and performed as previously reported (Ghoshal et al., 2001; Ghoshal et al., 2002). Briefly, digital images were captured using a Nikon Eclipse 800 light microscope coupled to a XC30 digital camera (Olympus Imaging America, Center Valley, PA, USA). All sections immunostained with one antibody were analyzed during a single session to minimize changes due to illumination, lamp intensity, or camera setting (Ghoshal et al., 2001; Ghoshal et al., 2002). From each region of interest (hippocampus, cortex, thalamus), digital images representing three non-overlapping fields (0.09mm^2) were captured. After each field was captured, the stage was moved manually to a new field using fiduciary landmarks, as determined by differential interference contrast (DIC) microscopy, to ensure non-redundant evaluation. Total immunoreactivity was estimated for each image by using the Set Threshold Function in the AnalySIS imaging software package (Olympus Soft Imaging Solutions, Lakewood, CO, USA). The following light intensity thresholds were selected to maximize the signal-to-noise ratio and were applied uniformly to all digital images: 145 for ubiquitin, 150 for both GFAP and IBA-1. The Phase Analysis function reported the percentage of the entire field that was included within the threshold. This value is equivalent to the total percentage of immunoreactivity present per field.

Statistical analyses

Survival curves for *Grn*-/-, *Grn*+/-, and *Grn*+/+ mice were created using the product limit method of Kaplan and Meier and the Log-rank (Mantel-Cox) Test was used to statistically test survival differences among these genotypes using GraphPad Prism statistical software package (GraphPad Software, Inc., La Jolla, CA, USA). Data from an individual mouse were censored if death was not due to natural causes (e.g., malocclusion, abscesses, or euthanization).

In general, analysis of variance (ANOVA) models were used to analyze the behavioral data. Typically, ANOVA models used for each cohort included one between-subjects variable (Genotype), and one within-subjects variable such as Blocks of Trials. Some models included two within-subjects variables such as trials and test sessions. The between-subjects variable, Gender, was included in the ANOVAs used to analyze the water maze data when both cohorts were combined since increased numbers for both sexes provided adequate power to analyze this variable. When ANOVAs with repeated measures were conducted, the Huynh-Feldt adjustment of alpha levels was used for all within-subjects effects containing more than two levels in order to help protect against violations of the sphericity/compound symmetry assumptions underlying this ANOVA model. Bonferroni correction was used to help maintain alpha levels at 0.05 when multiple comparisons were conducted.

Statistical analyses for quantitative immunohistochemistry involved measuring percent thresholds from three non-overlapping fields ($0.09mm^2$) as recorded by digital images which were examined for each mouse and each antibody; the analyses were based on the three-field averages. Unpaired t-test with Welch's correction was used to statistically test differences between *Grn*-/- and *Grn*+/+ mice using GraphPad Prism statistical software package (GraphPad Software, Inc., La Jolla, CA, USA) (Ghoshal et al., 2001; Ghoshal et al., 2002).

Results

Grn mice breeding, survival, and housing

Grn+/- mice were crossbred to generate *Grn*+/+, *Grn*+/-, and *Grn*-/- at the expected Mendelian distribution of 25, 50, 25%, respectively. Predicted Mendelian distribution was achieved in the colony. *Grn*+/+ offspring represented 25% of the pups (n=38 of 152 pups). *Grn*+/- offspring represented 49% of the pups (n=75 of 152 pups). *Grn*-/- offspring represented 26% of the pups (n=39 of 152 pups). Differential survival was noted among the genotypes such that *Grn*+/+ had median survival of 761 days (n=5) and *Grn*+/- had median survival of 803 days (n=42); whereas, *Grn*-/- had median survival of 514 days (n=25) (Fig. 1). 50% survival for *Grn*+/+ was 746 days, 791 days for *Grn*+/-, and 502 days for *Grn*-/- mice. The survival curves were significantly different ($p<0.0001$). Other than showing decreased overall survival, *Grn*-/- mice did not require any special consideration in terms of housing or handling. They could easily be group housed and were able to tolerate standard handling in the barrier facility. Initially, based on other groups' observations, we delayed obtaining genomic DNA from tail clips to postnatal day 21. However, upon returning to our standard operating procedure of procuring tails on postnatal day 5, no change in *Grn*-/- survival was noted. Our experience differs markedly from another group examining these mice (Ahmed et al., 2010) in terms of achieving Mendelian distribution, decreased survival of elder *Grn*-/- mice, and normal housing and handling protocols without adverse outcomes.

Changes in sample sizes due to attrition during the behavioral studies [See Supplemental Results].

Grn-/- mice exhibited normal levels of locomotor activity

Results from ANOVAs conducted on the activity data from the *Grn-/-* and *Grn+/+* mice in the first cohort (Fig. 2A-B, left panels) showed that the groups did not differ significantly with regard to general ambulatory activity (total ambulations) or exploratory behavior (vertical rearing frequency). In addition, the *Grn-/-* and *Grn+/+* groups exhibited significant decreases in total ambulations across the test session (Block 1 vs Block 6; $p < 0.0003$) thus demonstrating habituation. Similarly, the *Grn-/-* and *Grn+/+* mice also showed significant habituation across the session for rearing frequency ($p = 0.024$ and 0.003, respectively). Also, no differences were observed between groups with regard to the emotionality variables (time spent, distance traveled, or entries made into the center of the test field).

Similar results were found concerning the activity data from the second cohort in that no significant differences were observed between the *Grn-/-* and *Grn+/+* mice concerning total ambulations or rearings (Fig. 2A-B, right panels), and that both groups showed significant habituation in total ambulations across the session ($p < 0.0002$). However, both groups of mice exhibited lower levels of rearing particularly during the early time blocks and both the *Grn+/+* and *Grn-/-* mice showed smaller decreases in rearing from Block 1 to Block 6 than were observed in the younger cohort ($p = 0.038$ and $p > 0.05$, respectively). [See Supplemental Results for ANOVA details from these and other tests.]

Grn-/- mice showed intact sensorimotor capabilities except for impaired performance on the inverted screen test in the older, second cohort

No significant differences were found between groups in the younger cohort for any of the six measures within the sensorimotor battery similar to that shown in graphs depicting the data for the ledge test (Fig. 2C-D, left panels). This was also true for the second, older cohort except for the inverted screen test (Fig. 2C-D, right panels) where the *Grn-/-* mice remained hanging upside down on the screen for a significantly shorter period of time, [$F(1,22) = 11.07$, $p = 0.003$], relative to the *Grn+/+* controls.

Grn-/- mice were less reactive to handling than Grn+/+ controls

An ANOVA of the reactivity to handling data showed that, on average across test sessions, the *Grn-/-* male mice were hyporeactive to handling ($p = 0.009$), compared to *Grn+/+* males (Fig. 3A), and that reactivity to handling scores generally decreased over the test sessions ($p < 0.0005$). Subsequent pairwise comparisons showed that significant differences (Bonferroni corrected; $p < 0.05/3 = 0.017$) were observed during session 3 ($p = 0.013$), while large differences were also observed during session 2 ($p = 0.020$).

Grn-/- mice showed diminished social interactions rather than heightened aggression on the resident-intruder test

No significant differences were observed between the *Grn-/-* and *Grn+/+* mice on an index of aggression (fighting + biting durations) across the test sessions (Fig. 3B). However, compared to *Grn+/+* mice, the *Grn-/-* group showed significantly shorter duration of pawing (Fig. 3C) during nonaggressive interactions ($p = 0.005$), with significant differences being observed during session 3 ($p = 0.004$), although large differences were also observed during sessions 1 ($p = 0.018$) and 2 ($p = 0.021$). The *Grn-/-* mice were also found to follow the intruder mouse for a significantly shorter duration of time (Fig. 3D) compared to the *Grn +/+* controls ($p = 0.018$). This effect was mostly due to significant differences being observed during session 3 ($p = 0.004$). The *Grn-/-* group also spent a significantly greater amount of time alone (Fig. 3E) compared to the *Grn+/+* mice, ($p = 0.004$), and the effect of Test Session was significant as well ($p = 0.0027$), suggesting that the time spent alone was different across sessions. Pairwise comparisons showed that differences between groups

were significant during sessions 1 ($p = 0.006$) and 2 ($p= 0.012$), while differences were also large during session 3 ($p = 0.026$).

Grn-/- and Grn+/+ mice show similar olfactory preferences across different odorants

Results from the holeboard olfactory preference test indicated that the *Grn*-/- and *Grn*+/+ mice in the second (older cohort) had similar levels of general hole poking (data not shown) and exhibited similar hole poking preferences for a familiar odorant (fresh bedding), and a familiar food odorant (cereal) when tested under food restricted conditions, although neither group showed a preference for a novel odorant (coconut extract) (Fig. 4). Planned contrasts conducted within each group for the familiar odorant data showed that, on average, both the *Grn*-/- and *Grn*+/+ mice made significantly greater numbers of pokes into the holes containing bedding versus the empty holes ($p = 0.0001$ and 0.044, respectively) (Fig. 4A). In contrast, neither the *Grn*-/- nor the *Grn*+/+ mice poked significantly more often into the novel odorant versus the empty holes (Fig. 4B). However, both the *Grn*-/- and the *Grn*+/+ mice poked significantly more frequently into the holes that contained a familiar food odorant versus the empty holes ($p < 0.00005$) when the mice were tested following overnight (20-h) fasting (Fig. 4C). These data suggest that the *Grn*-/- mice had at least relatively normal olfactory functions.

Grn-/- mice show mild spatial (place) learning and memory deficits in the Morris water maze

Analysis of the cued trials data revealed that there were no significant overall effects involving either Genotype or Gender with regard to escape path length (Fig. 5A) or latency, or swimming speeds (data not shown), suggesting that the *Grn*-/- mice did not have impairments in non-associative functions that would affect their swimming performance in the subsequent place trials. In contrast, an ANOVA on the path length data from the place condition (Fig. 5B) showed that the acquisition performance of the *Grn*-/- group was significantly impaired relative to the *Grn*+/+ control mice ($p = 0.012$). Differences between groups were significant for block 3 ($p = 0.005$) with large differences also being observed during blocks 2 ($p = 0.033$) and 5 ($p = 0.018$). Differences between groups were even greater for escape latency (data not shown) although differences in swimming speeds (Fig. 5C) indicated that latency was not appropriate for evaluating acquisition performance. Specifically, an ANOVA on the swimming speeds revealed that the *Grn*-/- mice swam significantly more slowly, on average across the blocks of trials, relative to the *Grn*+/+ group ($p = 0.0001$).

The *Grn*-/- mice also showed impaired retention performance compared to the *Grn*+/+ mice during the probe trial in terms of platform crossings, ($p = 0.045$), suggesting that the *Grn*-/- mice had less reliable retention of the exact location of where the platform had been (Fig. 5D). However, the *Grn*-/- group performed as well as *Grn*+/+ mice with regard to less highly resolved indices of retention such as time spent in the target quadrant and spatial bias (Fig. 5E). Moreover, additional analyses showed that both groups demonstrated a spatial bias for the target quadrant by spending significantly more time in it relative to the times spent in the other quadrants ($p < 0.00005$).

No overall effects involving Gender were found for any of the place or probe trial variables. Importantly, additional ANOVAs on the place and probe trial data, which included the variables of Genotype, Cohort, and Blocks of Trials showed that there were no significant overall effects involving Cohort, including any interactions, thus justifying the combination of the cohorts.

Grn-/- mice displayed a general acquisition deficit on a learning set water maze task

Planned comparisons conducted on the escape path lengths of the *Grn*-/- and *Grn*+/+ mice from the older cohort showed they did not differ significantly on trial 2 (Fig. 6A), and neither group improved their averaged performance from trial 1 to trial 2. This suggested that training was not extensive enough for either group to demonstrate good working memory performance. However, the groups did differ in terms of general daily acquisition performance (trial 1 vs trial 4), which was analyzed in two ways. One analysis involved an ANOVA containing Genotype and Trial collapsed across test days (Fig. 6A) which yielded a significant effect of Trial, ($p = 0.048$). Subsequent contrasts indicated that the *Grn*+/+ mice significantly improved their performance from trial 1 to trial 4 ($p = 0.024$) suggesting some acquisition of the learning set task, while the *Grn*-/- mice showed no significant improvement.

To provide an additional assessment of each group's daily acquisition performance on the learning set task, another ANOVA was conducted within each group, which contained two within-subjects variables [trial 1 vs trial 4; and test days (1-5)]. The results of this analysis for the *Grn*-/- group, showed a significant effect of Test Day, ($p < 0.00005$), although the effect of Trial was not significant (Fig. 6B), suggesting that set learning did not occur. In contrast, we found significant effects for both Test Day, ($p = 0.0016$), and more importantly, a significant effect of Trial ($p = 0.047$), for the *Grn*+/+ mice (Fig. 6C), documenting significantly improved performance in the control mice suggesting that learning had occurred. Thus, only the *Grn*+/+ mice showed evidence of having acquired the learning set task.

Neuropathology

We observed no macroscopic brain changes in the *Grn-/-* mice. Microscopy was undertaken using standard stains and a panel of antibodies to detect the most commonly encountered molecular pathologies seen in neurodegenerative diseases. In the *Grn-/-* mice we observed a marked increase in the number of ubiquitinated structures (the fine structure of these is the focus of a separate study), largely in the neuropil and a pronounced glial reaction including microglial activation (increase in cell body size and number of ramified processes) and astrogliosis (increase in cell body size, increase in GFAP-immunoreactivity, and increase in size and number of astrocytic processes (Figs. 8 and 9; and see below). In the *Grn-/-* mice there was no evidence, in multiple cortical and subcortical nuclei, of β-amyloidosis, tauopathy, α-synucleinopathy, or TDP-43 proteinopathy. None of the compact neuronal TDP-43-immunoreactive cytoplasmic inclusions (NCI), neuronal intranuclear inclusions (NII), dystrophic neurites (DN), or glial inclusions commonly seen in FTLD with *Grn* mutation were present (Armstrong et al., 2011).

Neuron density

Unbiased stereology was used to estimate the density of neurons in the hippocampus, cortex, and thalamus in a section adjacent to those used to assess markers of gliosis, ubiquitination, and other markers of pathology associated with FTLD with *GRN* mutation. Using the optical fractionator and Cavielieri's estimate of the area of interest, the neuronal density, N_v (cells/mm^3), was calculated. The density of neurons in the dorsal thalamus of the *Grn-/-* mice was less than that of the *Grn*+/+ mice (115,400 ± 5,000 and 141,200 ± 16,000 neurons/mm^3 (mean ± SEM), respectively), but this was a non-significant trend in the relatively small number of mice available ($p = 0.17$). No differences were found between the estimates of the sample volume and neuron number in *Grn-/-* and *Grn*+/+ mice in the cortex (222,400 ± 11,400 and 198,000 ± 9,700 neurons/mm^3 (mean ± SEM; $p = 0.16$), respectively) or the CA1 subfield of the hippocampus (151,400 ± 58,400 and 148,100 ± 21,000 neurons/mm^3 (mean ± SEM); $p = 0.95$), respectively.

Ubiquitin immunoreactivity is increased in elder Grn-/- mice

To investigate the pathological substrate of the social behavior and memory deficits in *Grn-/-* and *Grn+/+* mice, FTLD-related brain changes were investigated. No discernible changes were detected by 10 weeks of age (data not shown). However, at 21.5 months (comparable to a 70-year-old human (Turnbull et al., 2003)), gliosis (microglia activation and reactive astrocytosis) was detected in *Grn-/-* relative to *Grn+/+* mice. At that age, increased ubiquitin-immunoreactivity was noted in the *Grn-/-* frontal lobes in the form of parenchymal ubiquitin-positive grains and dystrophic neurites and granular neuronal cytoplasmic inclusions (NCI). To evaluate these findings further, a group of 24 month old mice (comparable to an 80-year-old human *Grn+/+* (n=4) and *Grn-/-* (n=4) were assessed.

The most pronounced morphological changes in the *Grn-/-* mice were: extracellular ubiquitin-immunoreactive grains, a few foamy macrophages containing ubiquitin immunoreactivity, and rare neuronal cytoplasmic aggregates of ubiquitin-positivity; no compact fibrillary inclusion bodies were seen (Fig. 7). In the hippocampus, densitometry revealed significantly increased ubiquitin immunoreactivity in *Grn-/-* mice as compared to age-matched *Grn+/+* mice ($p = 0.0002$). There was increased cytoplasmic ubiquitin-immunoreactive granularity in the *Grn-/-* neurons and an occasional NCI was seen. In the cortex, the ubiquitin staining in *Grn-/-* mice was quantitatively comparable to *Grn+/+* ($p = 0.1179$). However, the staining in *Grn-/-* mice included parenchymal ubiquitin-immunoreactive grains and neurites which were rarely seen in the age-matched *Grn+/+* mice. In the thalamus, there was significantly increased ubiquitin-immunoreactivity in *Grn-/-* versus *Grn+/+* mice ($p = 0.0012$). The ubiquitin-immunoreactivity in *Grn-/-* thalamus was a combination of extracellular grains and neurites and cytoplasmic aggregates of varying forms. Notably, the most predominant intensely stained structures in the region were ubiquitin-positive grains/neurites in the brain parenchyma (Fig. 7). The increased ubiquitination in *Grn-/-* mice was also accompanied by neuronal vacuolation comparable to the observations of Ahmed and colleagues (Ahmed et al., 2010) although we did see a modest reduction in dorsal thalamic neurons this did not reach statistical significance.

Microglial activation in elder Grn-/- mice

Microglial activation was assessed using a marker of activated microglia (IBA-1). In the hippocampus, there was proliferation of microglia/macrophages in the *Grn-/-* mice as compared to the age-matched *Grn+/+* mice ($p=0.0421$). Activated microglia were also present in the cortex ($p=0.0019$) and thalamus ($p=0.0011$). In the three regions of interest, the microglia were increased in number and degree of arborization among *Grn-/-* mice. As with the increase in ubiquitin-immunoreactivity in the thalamus, microglial activation was most marked in the thalamus (Fig. 8).

Astrocytosis in elder Grn-/- mice

Astrocytosis was assessed by quantitative GFAP densitometry. In the hippocampus, there was increased astrocytosis in the *Grn-/-* mice as compared to the age-matched *Grn+/+* mice ($p<0.0001$). The degree of astrocytosis was statistically just as robust in the cortex ($p<0.0001$) and thalamus ($p<0.0001$). However, the absolute burden of astrocytosis was markedly more in the thalamus (Fig. 9).

Absence of TDP-43 proteinopathy in elder Grn-/- mice

While FTLD with *GRN* mutation is typified by TDP-43-immunoreactive inclusions, no TDP-43-immunoreactive inclusions (neuronal or glial) were detected in the elder *Grn-/-* mice. In particular, we looked at multiple, cortical, subcortical, brain stem, and cerebellar nuclei, including the dentate fascia, but found no discrete granular or filamentous inclusion

bodies with either phosphorylation-independent or phosphorylation-dependent anti-TDP-43 antibodies. In addition, no lesions were identified which were tau, α-synuclein, FUS, or β-amyloid-positive.

Discussion

Our results show that middle-aged and older *Grn*-/- mice (comparable to the age at onset in FTD (Turnbull et al., 2003)) have a phenotype that qualifies them as a useful model of frontotemporal dementia. Behavioral characteristics of our middle-aged *Grn*-/- male mice include an absence of elevated aggressiveness in contrast to the presence of hyperaggressiveness reported in juvenile *Grn*-/- males (Kayasuga et al., 2007). The middle-aged *Grn*-/- male mice of our colony also exhibited behavioral patterns that were interpreted as representing reduced levels of social engagement. Our data also suggest that older middle-aged *Grn*-/- mice have cognitive impairments such as mild learning and memory deficits. These behavioral characteristics combined with our neuropathological findings of neurodegeneration, increased ubiquitin-immunoreactivity, microglial activation and reactive astrocytosis in aged *Grn*-/- mice support the utility of the *Grn*-/- mouse model of frontotemporal dementia.

Although the *Grn*-/- and *Grn*+/+ mice exhibited similar levels of aggressiveness, there were robust differences on other more socially-oriented indices of the resident-intruder test (pawing, following, time spent alone), which showed that the *Grn*-/- mice interacted much less frequently with the young intruder males compared to the *Grn*+/+ group. The results from the reactivity to handling test indicated that the *Grn*-/- males were somewhat hyporeactive to handling suggesting diminished aggressiveness in this situation. Since there were no differences in the levels of locomotor activity or exploratory behaviors between *Grn*-/- and *Grn*+/+ mice, these results may indicate a possible lack of interest in, or awareness of, possibly threatening environmental events on the part of the *Grn*-/- mice. The consistent lack of differences between *Grn*-/- and *Grn*+/+ mice in the older cohort across different types of odorants argues against the existence of olfactory abnormalities being responsible for a lack of increased aggressiveness in the *Grn*-/- mice. Additional studies including formal social behavioral analyses are needed to clarify the phenotype of *Grn*-/- mice.

The Morris water maze and learning set results indicate mildly impaired learning and memory performance in the *Grn*-/- mice that this is likely due to cognitive deficits. Specifically, the *Grn*-/- mice exhibited significantly longer escape path lengths in navigating to the submerged platform during acquisition training in the place (spatial learning) condition. The *Grn*-/- mice also exhibited probe trial deficits in terms of platform crossings, a measure which represents a relatively highly resolved retention of the platform location. However, the *Grn*-/- mice were not impaired on more generalized aspects of retention such as time spent in the target quadrant or spatial bias for the target quadrant. These water maze results suggest that *Grn*-/- mice have mild acquisition deficits and slightly less precise retention of the platform location, although they eventually showed signs of reference-memory-based spatial learning. Further evidence of compromised cognitive function in the *Grn*-/- mice comes from the water maze learning set data collected in the older cohort of mice. These results indicated that the *Grn*+/+ control mice showed significantly improved performance from trial 1 to trial 4, demonstrating some acquisition of the learning set task while the *Grn*-/- mice showed no such evidence of learning. Since neither group displayed improved performance from trial 1 to trial 2, our learning set results should not be construed as a demonstration that *Grn*-/- mice have “normal” working (trial-dependent) memory capabilities. Additional studies that allow for a demonstration of learning in working-

memory-based tasks in *Grn*+/+ mice are required to evaluate this type of memory in *Grn*-/- mice.

One might argue that since the *Grn*-/- mice swam significantly more slowly in the place condition, their impaired acquisition performance may have reflected sensorimotor disturbances rather than cognitive deficits. Based on the inverted screen test it seems that older *Grn*-/- mice had minor sensorimotor dysfunction such as reduced grip strength, but this did not produce any impairments on the other six sensorimotor measures or alter the locomotor activity/exploratory behavior of the *Grn*-/- mice. More importantly, the nearly identical escape path lengths of the *Grn*-/- and *Grn*+/+ mice during the cued trials suggest that if the *Grn*-/- mice had a sensorimotor disturbance, it did not affect their swimming performance in that they were able to demonstrate control-like levels of cued learning performance. Since the groups did not differ on any of the cued trials variables, it is difficult to attribute any non-associative dysfunction in the *Grn*-/- mice (visual, sensorimotor, or motivational disturbances) as being responsible for the spatial learning performance deficits. Additional evidence supporting the idea that *Grn*-/- mice have cognitive impairments comes from the learning set data where the critical analyses involved within-subjects comparisons (i.e., trial 1 vs trial 4) with regard to path length in each group. Therefore, differences in swimming speeds between groups should not have affected the outcomes of these contrasts. Confidence in our results has been strengthened by comparable behavioral findings (impaired social interaction and cognition) that have been recently reported in a conditional *Grn* knockout mouse model using the Cre-lox system to delete the promoter and exons 1-4 (Yin et al., 2009; Yin et al., 2010).

In an effort to understand the neurological basis for the behavioral phenotype of the *Grn*-/- mouse and to evaluate its utility in serving as a model of FTLD, we conducted various histopathological analyses and found lesions pathognomonic for FTLD with *GRN* mutation. Increased ubiquitination, microgliosis, and astrocytosis were found in *Grn*-/- mice in all regions of interest: hippocampus, cortex, and thalamus. These lesions were present in 12 month old *Grn*-/- mice and to a significantly greater degree in the 24 month old *Grn*-/- mice. The pathological changes seen in the *Grn*-/- mice correlate well with the behavioral changes that were noted beginning at 9-12 months of age. The age-dependent increase in these lesions has been shown by another group working with this particular *Grn* model (Ahmed et al., 2010). However, there are key differences that are likely due to colony effects since Ahmed et al experienced deviations from the Mendelian distribution in their *Grn*-/- mouse breeding program. In addition, their *Grn*-/- mice were particularly sensitive to handling resulting in heightened postnatal death, which was not the case with our mice (Ahmed et al., 2010).

Notably, one signature lesion of FTLD with *GRN* mutation, TDP-43 proteinopathy, was not seen in this murine model. This could be because these mice were not yet old enough to demonstrate TDP-43 inclusions or even nuclear-cytoplasmic translocation. However, given that the pathologic analyses were conducted on 24-month-old mice (comparable to an 80-year-old human (Turnbull et al., 2003)), it is unlikely that the mice would survive much longer to develop TDP-43 proteinopathy. The lack of TDP-43 proteinopathy has also been shown by two other groups using these mice, albeit at somewhat younger ages than investigated here (Ahmed et al., 2010; Dormann et al., 2009). There are other instances in which progranulin deficiency has not resulted in TDP-43 pathology. In one study, progranulin was acutely knocked down in zebrafish without causing a reduction in nuclear staining or increased cytoplasmic staining of TDP-43 (Shankaran et al., 2008). In another study, *GRN* knockdown in HeLa and SH-SY5Y cells failed to induce caspase activation and proteolytic cleavage of full-length TDP-43 into the 35 kDa C-terminal fragments (CTF) associated with FTLD with *GRN* mutation (Dormann et al., 2009). These studies suggest

that perhaps TDP-43 proteinopathy (nuclear clearance and cytoplasmic aggregation, phosphorylation, and C-terminal cleavage) are not necessary for disease. Additional evidence comes from the first mutant TDP-43 transgenic mouse in which a clear motor neuron disease phenotype developed at 3 months accompanied by ubiquitinated cytoplasmic inclusions but not TDP-43 inclusions (Wegorzewska et al., 2009). The TDP-43 mouse model suggests that TDP-43 aggregates are perhaps not necessary for neurodegeneration (Wegorzewska et al., 2009). However, one other *Grn*-deficient mouse model has demonstrated phosphorylated, cytoplasmic TDP-43 *in situ* (Yin et al., 2009). Furthermore, TDP-43 cytoplasmic accumulations have been reported in two *Grn*-deficient mouse primary cortical neuron systems (Guo et al., 2010; Kleinberger et al., 2010).

The brain regions in which histopathological markers and lesions were documented provide possible substrates for the behavioral impairments observed in *Grn-/-* mice. For example, it is reasonable to predict that neuropathological changes in the hippocampus and fronto-temporal cortical regions are likely to contribute to the learning/memory deficits and abnormal social behaviors, respectively, in *Grn-/-* mice. Although less well appreciated, thalamic damage may also play a role in the cognitive disturbances. For example, thalamic lacunes may contribute to cognitive decline independent of Alzheimer's disease pathology (Gold et al., 2005), and thalamic atrophy is a clinically relevant biomarker of multiple sclerosis (Houtchens et al., 2007) and Alzheimer's disease (de Jong et al., 2008). Important information relevant to this mouse model of FTD may be provided by future studies that focus on whether *Grn*-/- mice show an additional accelerated decline in cognitive capabilities and/or other behavioral changes in advanced age when neuropathological markers become conspicuous.

A key finding in this study was that *Grn*-/- mice have decreased survival. This, to our knowledge, has not previously been reported for this murine model of FTD. There was no alteration in the Mendelian inheritance pattern and, therefore, the differences cannot be attributed to embryonic or early-life deaths. Even the *Grn*-/- mice had a median survival of 514 days, which is consistent with a disorder occurring in later life. The *Grn*-/- mice did not appear to suffer from ailments at a greater rate than their *Grn*+/- and *Grn*+/+ siblings. Findings from another *Grn*-deficient mouse model offer some insights into the differential survival observed in the current study. Yin et al. found their *Grn*-deficient mice to have exaggerated inflammation and impaired host defense mechanisms (Yin et al., 2009). The *Grn*-deficient brains showed a failure to clear infection quickly with resultant bacterial proliferation and greater inflammation than seen in the wild type. No survival data were provided to conclude definitively that dysregulated inflammation resulted in differential survival of their mice. When reviewing human FTD survival data, it appears that hereditary forms of the disease are more aggressive in their course than sporadic FTD such that mean disease duration of FTD patients with negative family history has been reported at 9.9 years versus 8.4 years in FTD patients with positive family history (Chiu et al., 2010). In the same study, patients with *GRN* mutation had a survival of 7.7 years (Chiu et al., 2010).

The *Grn*-/- murine model described in detail in the current study recapitulates key aspects of FTD in terms of behavior, pathology, and survival thus making it a useful model system to dissect the mechanism by which progranulin deficiency results in FTD behavioral symptoms and FTLD pathology. As novel targets and therapies are developed, this model will provide a well-defined system in which future therapeutics can be screened and tested.

Supplementary Material

Refer to Web version on PubMed Central for supplementary material.

Acknowledgments

We thank Prof. Masugi Nishihara for providing us with the *Grn*-/- mice, Sara Conyers of the Washington University Animal Behavior Core for assistance with the behavioral testing, Deborah Carter of the Knight ADRC Neuropathology Core Laboratory for histology and immunohistochemistry, Cathy Roe of the Knight ADRC Biostatistics Core for guidance and supervision of the survival analyses. Support was provided by the National Institute on Aging of the National Institutes of Health: T32-NS007205 (NG); P01-AG003991 (NG, NJC) and P50-AG005681 (NG, NJC); an NIH Neuroscience Blueprint Interdisciplinary Center Core Grant P30-NS057105 to Washington University (DFW), and the Charles and Joanne Knight Alzheimer Research Initiative (NJC).

Support: T32-NS007205; P01-AG03991 (NG, NJC) and P50-AG005681 (NG, NJC); P30-NS057105 (DFW); Charles and Joanne Knight Alzheimer Research Initiative (NJC)

References

Ahmed Z, Sheng H, Xu YF, Lin WL, Innes AE, Gass J, Yu X, Hou H, Chiba S, Yamanouchi K, Leissring M, Petrucelli L, Nishihara M, Hutton ML, McGowan E, Dickson DW, Lewis J. Accelerated Lipofuscinosis and Ubiquitination in Granulin Knockout Mice Suggests a Role for Progranulin in Successful Aging. Am J Pathol. 2010

Armstrong RA, Carter D, Cairns NJ. A Quantitative Study of the Neuropathology of Thirty-Two Sporadic and Familial Cases of Frontotemporal Lobar Degeneration with Tdp-43 Proteinopathy (Ftld-Tdp). Neuropathol Appl Neurobiol. 2011

Baker M, Mackenzie IR, Pickering-Brown SM, Gass J, Rademakers R, Lindholm C, Snowden J, Adamson J, Sadovnick AD, Rollinson S, Cannon A, Dwosh E, Neary D, Melquist S, Richardson A, Dickson D, Berger Z, Eriksen J, Robinson T, Zehr C, Dickey CA, Crook R, McGowan E, Mann D, Boeve B, Feldman H, Hutton M. Mutations in progranulin cause tau-negative frontotemporal dementia linked to chromosome 17. Nature. 2006; 442:916–9. [PubMed: 16862116]

Bateman A, Bennett HP. The granulin gene family: from cancer to dementia. Bioessays. 2009; 31:1245–54. [PubMed: 19795409]

Behrens MI, Mukherjee O, Tu PH, Liscic RM, Grinberg LT, Carter D, Paulsmeyer K, Taylor-Reinwald L, Gitcho M, Norton JB, Chakraverty S, Goate AM, Morris JC, Cairns NJ. Neuropathologic heterogeneity in HDDD1: a familial frontotemporal lobar degeneration with ubiquitin-positive inclusions and progranulin mutation. Alzheimer Dis Assoc Disord. 2007; 21:1–7. [PubMed: 17334266]

Cairns NJ, Bigio EH, Mackenzie IR, Neumann M, Lee VM, Hatanpaa KJ, White CL 3rd, Schneider JA, Grinberg LT, Halliday G, Duyckaerts C, Lowe JS, Holm IE, Tolnay M, Okamoto K, Yokoo H, Murayama S, Woulfe J, Munoz DG, Dickson DW, Ince PG, Trojanowski JQ, Mann DM. Neuropathologic diagnostic and nosologic criteria for frontotemporal lobar degeneration: consensus of the Consortium for Frontotemporal Lobar Degeneration. Acta Neuropathol (Berl). 2007; 114:5–22. [PubMed: 17579875]

Chiu WZ, Kaat LD, Seelaar H, Rosso SM, Boon AJ, Kamphorst W, van Swieten JC. Survival in progressive supranuclear palsy and frontotemporal dementia. J Neurol Neurosurg Psychiatry. 2010; 81:441–5. [PubMed: 20360166]

Cruts M, Gijselinck I, van der Zee J, Engelborghs S, Wils H, Pirici D, Rademakers R, Vandenberghe R, Dermaut B, Martin JJ, van Duijn C, Peeters K, Sciot R, Santens P, De Pooter T, Mattheijssens M, Van den Broeck M, Cuijt I, Vennekens K, De Deyn PP, Kumar-Singh S, Van Broeckhoven C. Null mutations in progranulin cause ubiquitin-positive frontotemporal dementia linked to chromosome 17q21. Nature. 2006; 442:920–4. [PubMed: 16862115]

de Jong LW, van der Hiele K, Veer IM, Houwing JJ, Westendorp RG, Bollen EL, de Bruin PW, Middelkoop HA, van Buchem MA, van der Grond J. Strongly reduced volumes of putamen and thalamus in Alzheimer's disease: an MRI study. Brain. 2008; 131:3277–85. [PubMed: 19022861]

Dormann D, Capell A, Carlson AM, Shankaran SS, Rodde R, Neumann M, Kremmer E, Matsuwaki T, Yamanouchi K, Nishihara M, Haass C. Proteolytic processing of TAR DNA binding protein-43 by caspases produces C-terminal fragments with disease defining properties independent of progranulin. J Neurochem. 2009; 110:1082–94. [PubMed: 19522733]

Fabricius K, Wortwein G, Pakkenberg B. The impact of maternal separation on adult mouse behaviour and on the total neuron number in the mouse hippocampus. Brain Struct Funct. 2008; 212:403–16. [PubMed: 18200448]

Gallitano-Mendel A, Wozniak DF, Pehek EA, Milbrandt J. Mice lacking the immediate early gene Egr3 respond to the anti-aggressive effects of clozapine yet are relatively resistant to its sedating effects. Neuropsychopharmacology. 2008; 33:1266–75. [PubMed: 17637609]

Gass J, Cannon A, Mackenzie IR, Boeve B, Baker M, Adamson J, Crook R, Melquist S, Kuntz K, Petersen R, Josephs K, Pickering-Brown SM, Graff-Radford N, Uitti R, Dickson D, Wszolek Z, Gonzalez J, Beach TG, Bigio E, Johnson N, Weintraub S, Mesulam M, White CL 3rd, Woodruff B, Caselli R, Hsiung GY, Feldman H, Knopman D, Hutton M, Rademakers R. Mutations in progranulin are a major cause of ubiquitin-positive frontotemporal lobar degeneration. Hum Mol Genet. 2006; 15:2988–3001. [PubMed: 16950801]

Ghoshal N, Garcia-Sierra F, Fu Y, Beckett LA, Mufson EJ, Kuret J, Berry RW, Binder LI. Tau-66: evidence for a novel tau conformation in Alzheimer's disease. J Neurochem. 2001; 77:1372–85. [PubMed: 11389188]

Ghoshal N, García-Sierra F, Wuu J, Leurgans S, Bennett DA, Berry RW, Binder LI. Tau Conformational Changes Correspond to Impairments of Episodic Memory in Mild Cognitive Impairment and Alzheimer's Disease. Exp Neurology. 2002; 177:475–93.

Gold G, Kovari E, Herrmann FR, Canuto A, Hof PR, Michel JP, Bouras C, Giannakopoulos P. Cognitive consequences of thalamic, basal ganglia, and deep white matter lacunes in brain aging and dementia. Stroke. 2005; 36:1184–8. [PubMed: 15891000]

Gundersen HJ, Jensen EB. The efficiency of systematic sampling in stereology and its prediction. J Microsc. 1987; 147:229–63. [PubMed: 3430576]

Guo A, Tapia L, Bamji SX, Cynader MS, Jia W. Progranulin deficiency leads to enhanced cell vulnerability and TDP-43 translocation in primary neuronal cultures. Brain Res. 2010; 1366:1–8. [PubMed: 20888804]

Hartman RE, Lee JM, Zipfel GJ, Wozniak DF. Characterizing learning deficits and hippocampal neuron loss following transient global cerebral ischemia in rats. Brain Res. 2005; 1043:48–56. [PubMed: 15862517]

Houtchens MK, Benedict RH, Killiany R, Sharma J, Jaisani Z, Singh B, Weinstock-Guttman B, Guttmann CR, Bakshi R. Thalamic atrophy and cognition in multiple sclerosis. Neurology. 2007; 69:1213–23. [PubMed: 17875909]

Kayasuga Y, Chiba S, Suzuki M, Kikusui T, Matsuwaki T, Yamanouchi K, Kotaki H, Horai R, Iwakura Y, Nishihara M. Alteration of behavioural phenotype in mice by targeted disruption of the progranulin gene. Behav Brain Res. 2007; 185:110–8. [PubMed: 17764761]

Kleinberger G, Wils H, Ponsaerts P, Joris G, Timmermans JP, Van Broeckhoven C, Kumar-Singh S. Increased Caspase Activation and Decreased Tdp-43 Solubility in Progranulin Knockout Cortical Cultures. J Neurochem. 2010

Mackenzie IR, Neumann M, Bigio EH, Cairns NJ, Alafuzoff I, Kril J, Kovacs GG, Ghetti B, Halliday G, Holm IE, Ince PG, Kamphorst W, Revesz T, Rozemuller AJ, Kumar-Singh S, Akiyama H, Baborie A, Spina S, Dickson DW, Trojanowski JQ, Mann DM. Nomenclature and nosology for neuropathologic subtypes of frontotemporal lobar degeneration: an update. Acta Neuropathol. 2010; 119:1–4. [PubMed: 19924424]

McKhann GM, Albert MS, Grossman M, Miller B, Dickson D, Trojanowski JQ. Clinical and pathological diagnosis of frontotemporal dementia: report of the Work Group on Frontotemporal Dementia and Pick's Disease. Arch Neurol. 2001; 58:1803–9. [PubMed: 11708987]

Mesulam M, Johnson N, Krefft TA, Gass JM, Cannon AD, Adamson JL, Bigio EH, Weintraub S, Dickson DW, Hutton ML, Graff-Radford NR. Progranulin mutations in primary progressive aphasia: the PPA1 and PPA3 families. Arch Neurol. 2007; 64:43–7. [PubMed: 17210807]

Moy SS, Nadler JJ, Poe MD, Nonneman RJ, Young NB, Koller BH, Crawley JN, Duncan GE, Bodfish JW. Development of a mouse test for repetitive, restricted behaviors: relevance to autism. Behav Brain Res. 2008; 188:178–94. [PubMed: 18068825]

Mukherjee O, Pastor P, Cairns NJ, Chakraverty S, Kauwe JS, Shears S, Behrens MI, Budde J, Hinrichs AL, Norton J, Levitch D, Taylor-Reinwald L, Gitcho M, Tu PH, Tenenholz Grinberg L, Liscic

RM, Armendariz J, Morris JC, Goate AM. HDDD2 is a familial frontotemporal lobar degeneration with ubiquitin-positive, tau-negative inclusions caused by a missense mutation in the signal peptide of progranulin. Ann Neurol. 2006; 60:314–22. [PubMed: 16983685]

Neary D, Snowden JS, Gustafson L, Passant U, Stuss D, Black S, Freedman M, Kertesz A, Robert PH, Albert M, Boone K, Miller BL, Cummings J, Benson DF. Frontotemporal lobar degeneration: a consensus on clinical diagnostic criteria. Neurology. 1998; 51:1546–54. [PubMed: 9855500]

Paxinos, G.; Franklin, KBJ. The Mouse Brain in Stereotaxic Coordinates. Academic Press; London, UK: 2001.

Shankaran SS, Capell A, Hruscha AT, Fellerer K, Neumann M, Schmid B, Haass C. Missense mutations in the progranulin gene linked to frontotemporal lobar degeneration with ubiquitin-immunoreactive inclusions reduce progranulin production and secretion. J Biol Chem. 2008; 283:1744–53. [PubMed: 17984093]

Turnbull IR, Wlzorek JJ, Osborne D, Hotchkiss RS, Coopersmith CM, Buchman TG. Effects of age on mortality and antibiotic efficacy in cecal ligation and puncture. Shock. 2003; 19:310–3. [PubMed: 12688540]

Wegorzewska I, Bell S, Cairns NJ, Miller TM, Baloh RH. TDP-43 mutant transgenic mice develop features of ALS and frontotemporal lobar degeneration. Proc Natl Acad Sci U S A. 2009; 106:18809–14. [PubMed: 19833869]

Wozniak DF, Hartman RE, Boyle MP, Vogt SK, Brooks AR, Tenkova T, Young C, Olney JW, Muglia LJ. Apoptotic neurodegeneration induced by ethanol in neonatal mice is associated with profound learning/memory deficits in juveniles followed by progressive functional recovery in adults. Neurobiol Dis. 2004; 17:403–14. [PubMed: 15571976]

Yin F, Banerjee R, Thomas B, Zhou P, Qian L, Jia T, Ma X, Ma Y, Iadecola C, Beal MF, Nathan C, Ding A. Exaggerated inflammation, impaired host defense, and neuropathology in progranulin-deficient mice. J Exp Med. 2009

Yin F, Dumont M, Banerjee R, Ma Y, Li H, Lin MT, Beal MF, Nathan C, Thomas B, Ding A. Behavioral deficits and progressive neuropathology in progranulin-deficient mice: a mouse model of frontotemporal dementia. FASEB J. 2010

Highlights

- Characterization of a progranulin knockout mouse model of frontotemporal dementia.
- The mice exhibit reduced social engagement and learning and memory deficits.
- Pathology includes ubiquitination, microgliosis, and reactive astrocytosis.
- Progranulin knockout mice have decreased overall survival compared to wild type.
- These mice reflect key aspects of FTD in terms of behavior, pathology, and survival.

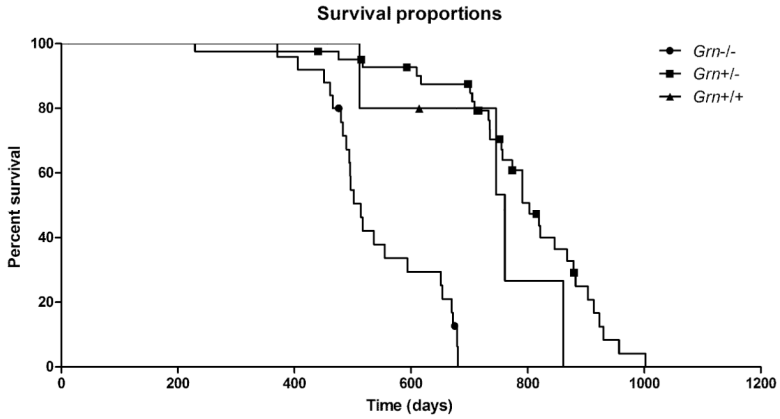

Fig. 1. Kaplan-Meier survival plots for *Grn* mice

Survival curve of *Grn*-/- mice showed a median survival of 514 days.

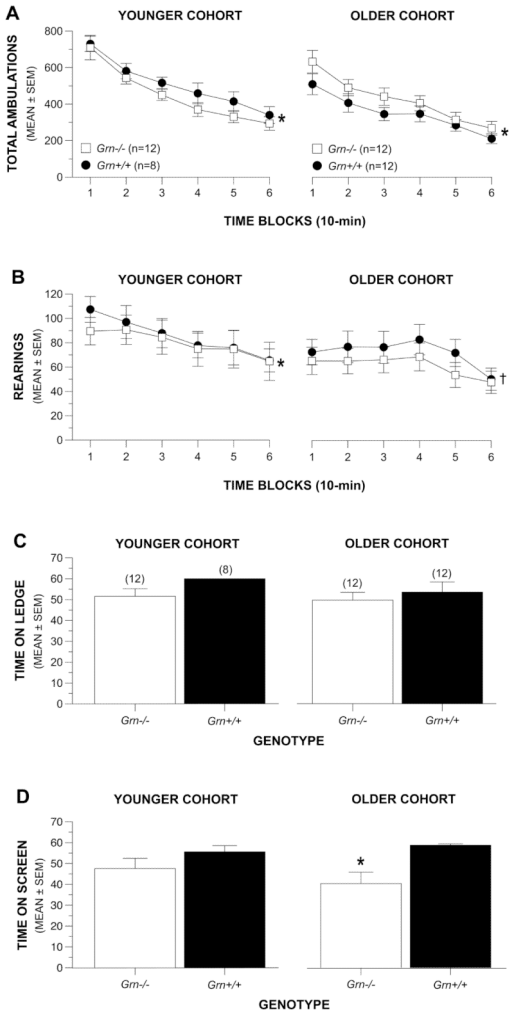

Fig. 2. *Grn*-/- mice displayed normal levels of locomotor activity and exploratory behavior and only mild sensorimotor deficits at older ages

(A) *Grn*-/- and *Grn*+/+ mice showed similar levels of general locomotor activity (total ambulations) in both younger (9-12 months) and older (15-18 months) cohorts. Both groups showed significant habituation of ambulatory activity over the test session in each cohort (*p < 0.0003). (B) The *Grn*-/- and *Grn*+/+ groups in both cohorts also showed similar levels of exploratory behavior in terms of vertical rearing. However, both groups showed significant habituation only in the younger cohort (*p = 0.025 and 0.003, respectively) while only the *Grn*+/+ mice showed evidence of habituation in the older cohort (†p = 0.038). (C) No differences were observed between the *Grn*-/- and *Grn*+/+ mice on 5 out of the 6 sensorimotor measures in either cohort similar to that represented in the data from the ledge test. Numbers in parentheses above bars represent sample sizes for each group. (D) However, although the groups performed similarly on the inverted screen test at an earlier age, the *Grn*-/- mice in the older cohort were significantly (*p = 0.003) impaired on the inverted screen test suggesting that they may have deficits in strength at this age.

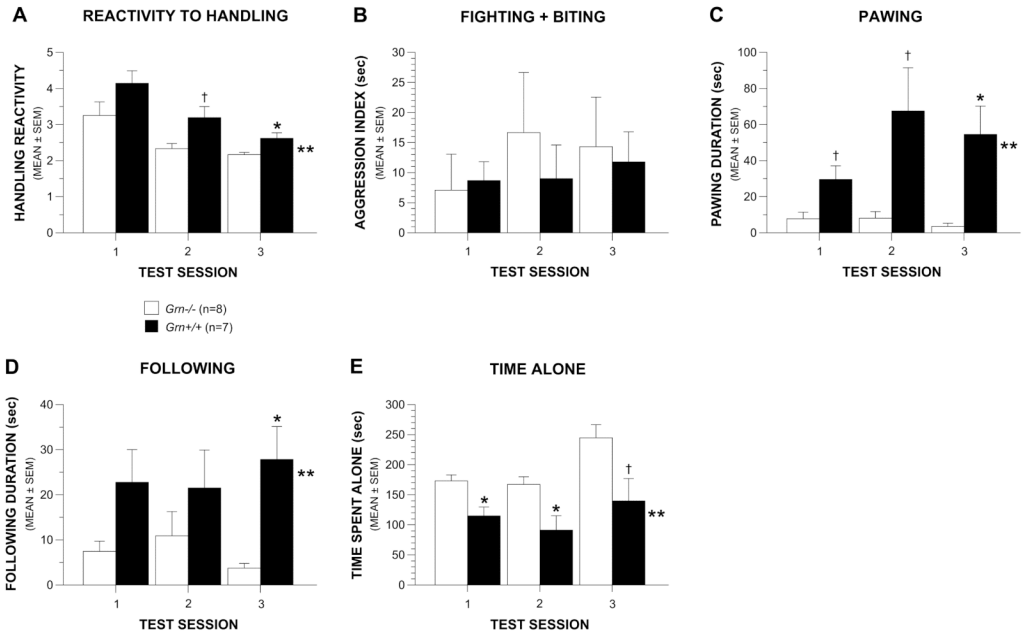

Fig. 3. *Grn*-/- male mice were not hyperaggressive but showed evidence of altered social interactions

(A) *Grn*-/- male mice were significantly less reactive to handling on average across three daily test sessions compared to *Grn*+/+ controls (**p = 0.009), with differences being significant during session 3 (*p = 0.013) and during session 2 (†p = 0.020). (B) However, no reliable differences were observed between the *Grn*-/- and *Grn*+/+ male groups on an aggression index (duration of fighting + biting) derived from data collected during the resident-intruder test. (C) In contrast, the *Grn*-/male mice displayed a significantly decreased duration of pawing during nonaggressive interactions (**p=0.005), with differences being significant during session 3 (*p = 0.004), and very large during sessions 1 and 2 (†p < 0.025). (D) Male *Grn*-/- mice also spent a significantly decreased duration of time following the intruder mouse compared to the *Grn*+/+ group across test sessions (**p = 0.018) with differences being significant during session 3 (*p = 0.004). (E) The *Grn*-/- mice spent significantly more time alone compared to the *Grn*+/+ group (**p = 0.004) with significant differences being observed during sessions 1 (*p = 0.006) and 2 (*p = 0.012) and substantial differences also being found for session 3 (†p = 0.026).

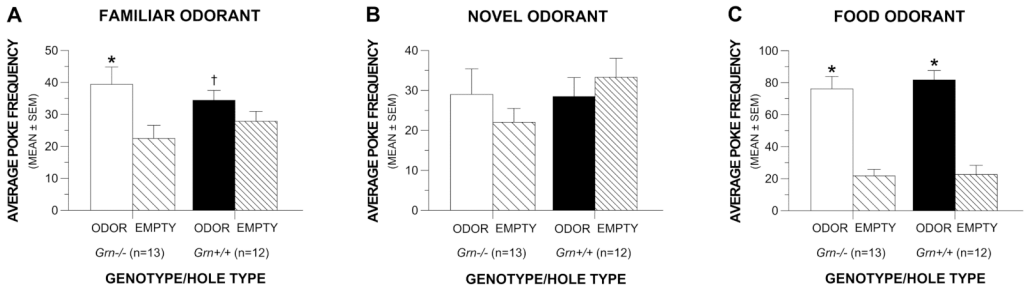

Fig. 4. *Grn*-/- and *Grn*+/+ mice showed similar olfactory preferences for different odorants

(A) The *Grn*-/- and *Grn*+/+ mice made more pokes into holes that contained fresh bedding, which was a familiar odorant (*p = 0.0001 and †p = 0.044, respectively), relative to empty holes. (B) However, neither group showed a significant preference for a novel odorant (coconut extract). (C) In contrast, the *Grn*-/- and *Grn*+/+ groups showed a striking preference for a familiar food odorant while under food-restricted conditions as indicated by both groups showing significantly increased levels of poking into the odorant holes compared to empty holes (*p < 0.00005).

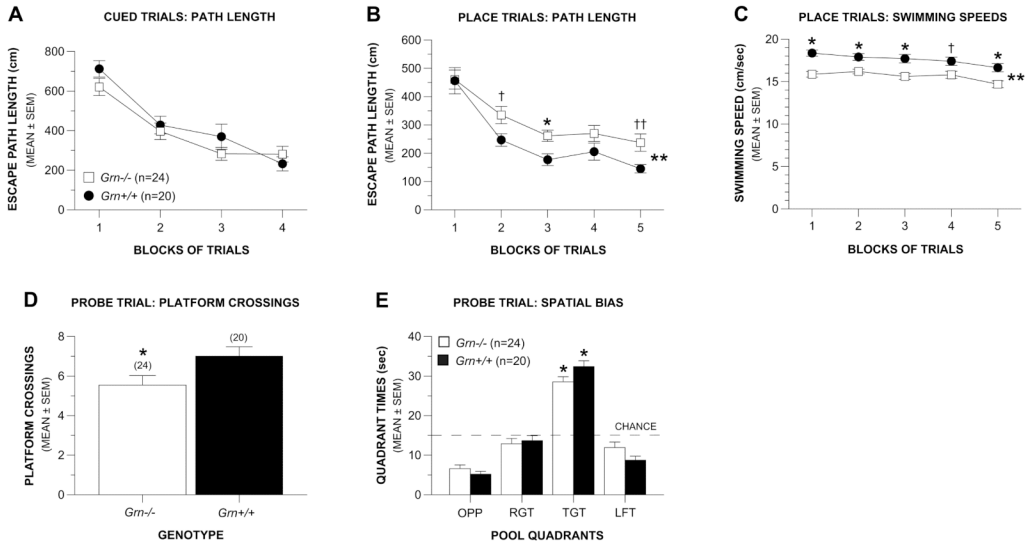

Fig. 5. *Grn-/-* mice exhibited mild spatial learning and memory deficits in the Morris water maze

(A) The *Grn-/-* and *Grn+/+* groups performed similarly in terms of escape path length during the cued trials in the water maze, suggesting that the *Grn-/-*mice did not have impaired nonassociative functions that would affect performance on the subsequent place condition. (B) However, on average across the blocks of trials, the *Grn-/-* mice showed significant acquisition deficits in terms of path length during the place trials compared to the *Grn+/+* controls (**p = 0.012). Differences were significant during block 3 (*p = 0.005), and very large during blocks 2 (†p = 0.033) and 5 (††p = 0.018). (C) The *Grn-/-* mice swam significantly more slowly on average across the blocks of trials compared to the *Grn+/+* control mice (**p = 0.0001), and differences between groups were significant for blocks 1, 2, 3, and 5 (*p < 0.003), and large for block 4 (†p = 0.015). (D) During the probe trial, the *Grn-/-* group made significantly fewer crossings over the location where the platform had been located compared to the *Grn+/+* mice (*p = 0.045) suggesting a deficit in the retention of the exact position of the platform. (E) However, the *Grn-/-* mice performed as well as *Grn+/+* controls on a less highly-resolved retention of the platform in terms of showing a significant spatial bias for the target quadrant that contained the platform. Both groups spent significantly more time in the target quadrant compared to each of the other pool quadrants (*p < 0.00005).

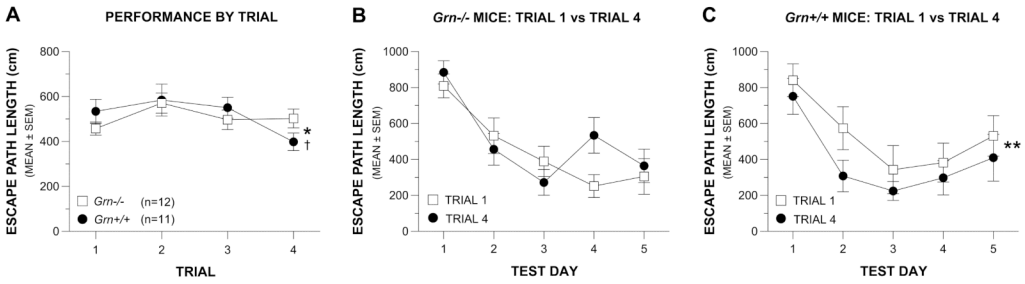

Fig. 6. *Grn-/-* mice displayed impaired acquisition performance on a learning set protocol in the water maze

(A) A significant effect of Trial was found with regard to the path length of the mice from the second cohort during the learning set protocol in the water maze, (*p = 0.048). In addition, a significant effect of Trial (1 vs 4) was found in the analysis of the data from the *Grn+/+* mice (†p = 0.024) but not from the *Grn-/-*group suggesting some acquisition of the learning set task in the *Grn+/+* mice but not in the *Grn-/-* group. (B) For the *Grn-/-* mice the effect of Trial (trial 1 vs trial 4) was not significant indicating that there was no improvement in performance from trial 1 to trial 4, although performance on both trials improved across test days. (C) In contrast, the effect of Trial was significant in the *Grn+/+* mice (**p = 0.047) showing that average path length was significantly decreased between trial 1 and trial 4 thus providing additional evidence for acquisition of the learning set task on the part of the *Grn+/+* controls.

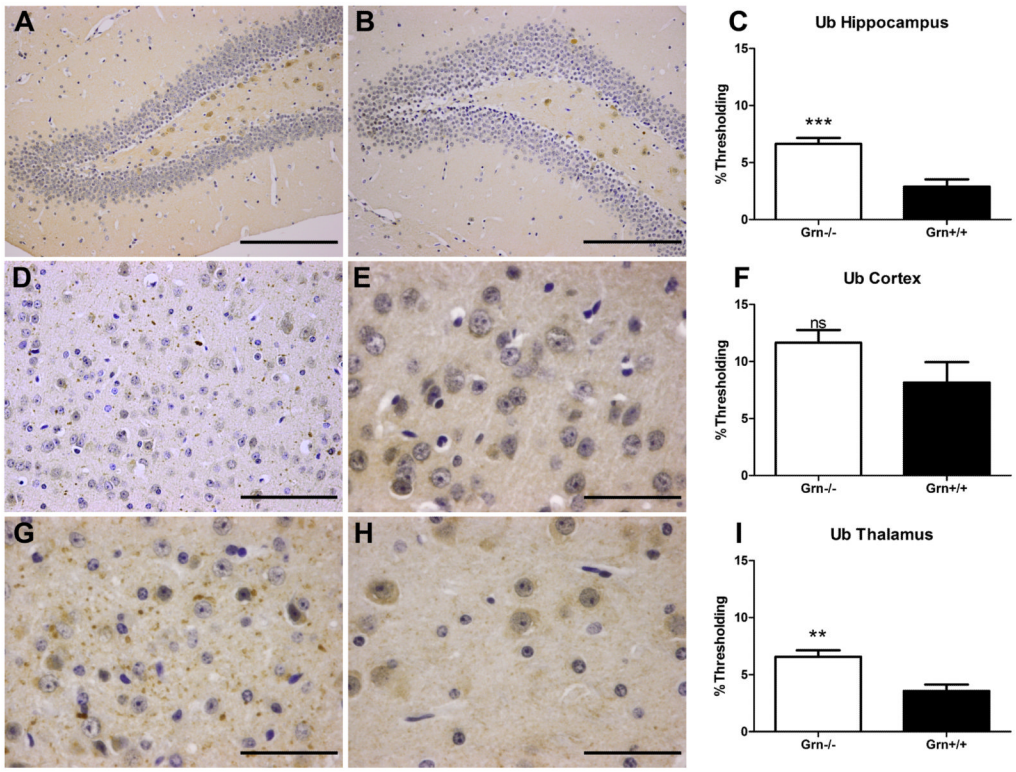

Fig. 7. Increased ubiquitination observed in 24-month old *Grn-/-* mice

Grn-/- mice (A, D, G; n=4) have an increased number of ubiquitinated structures, largely in the neuropil, compared to age-matched *Grn+/+* mice (B, E, H; n=4) in the (A-C) hippocampus, (D-F) cortex, and (G-I) thalamus. Scale bar 200 μm in (A, B), 100 μm in (D), 50 μm in (E), and 50 μm in (G, H). Percent thresholding shown in C, F, and I (*Grn-/-* in white, *Grn+/+* in black) as mean ± SEM. Statistics denoted as $p>0.05$, ns; $p<0.01$, **; and $p<0.001$, ***.

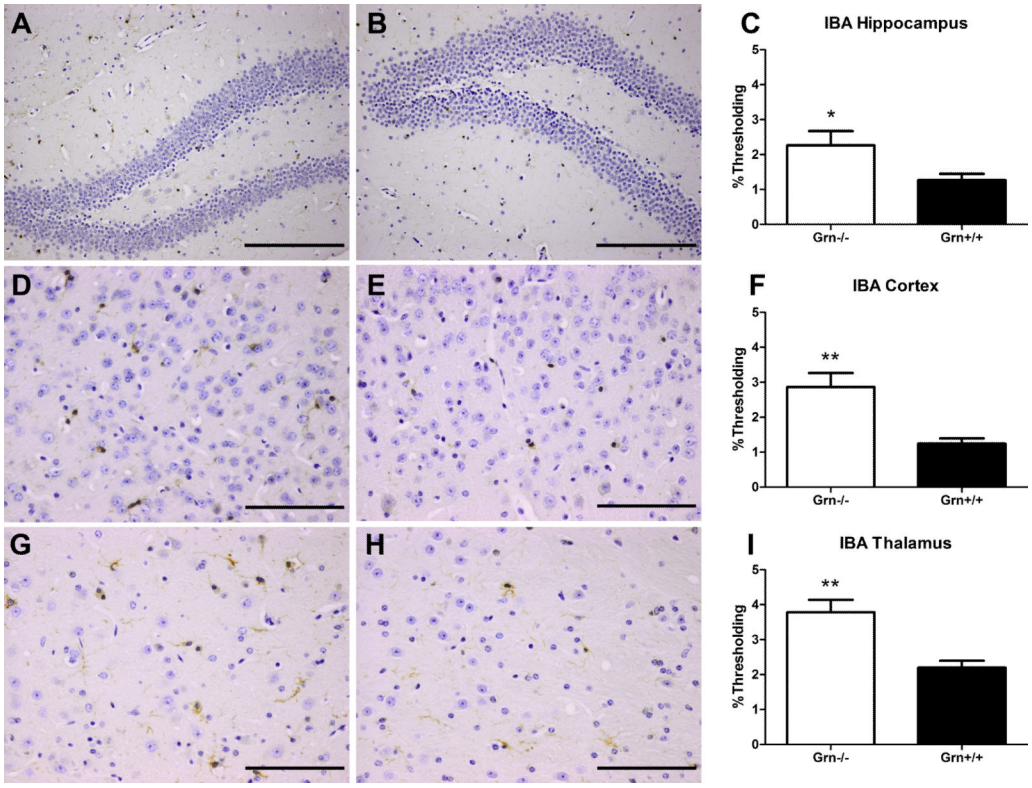

Fig. 8. Increased microgliosis observed in 24-month old *Grn-/-* mice

Grn-/- mice (A, D, G; n=4) have an increase in the number and size of IBA-1-immunoreactive microglial cells compared to age-matched *Grn*+/+ mice (B, E, H; n=4) in the (A-C) hippocampus, (D-F) cortex, and (G-I) thalamus. Scale bar 200 μm in (A, B), 100 μm in (D, E), and 100 μm in (G, H). Percent thresholding shown in C, F, and I (*Grn*-/- in white, *Grn*+/+ in black) as mean ± SEM. Statistics denoted as $p<0.05$, * and $p<0.01$, **.

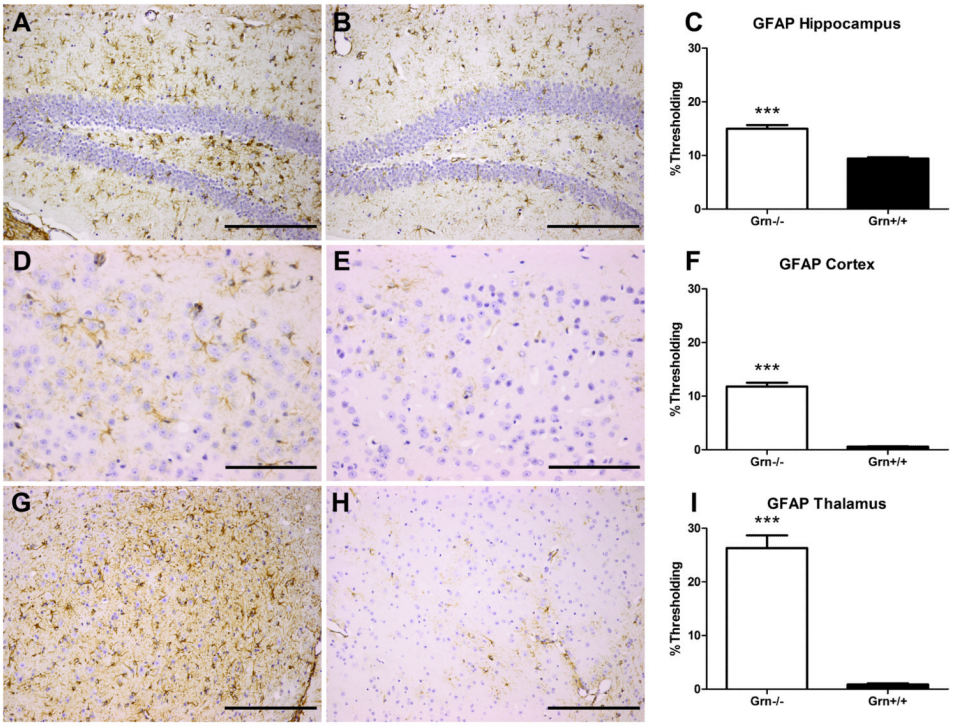

Fig. 9. Increased astrocytosis observed in 24-month old *Grn*-/- mice

Grn-/- mice (A, D, G; n=4) have increased GFAP immunoreactivity (number, cell body size, and number and size of processes) as compared to age-matched *Grn*+/+ mice (B, E, H; n=4) in the (A-C) hippocampus, (D-F) cortex, and (G-I) thalamus. Scale bar 200 μm in (A, B), 100 μm in (D, E), and 200 μm in (G, H). Percent thresholding shown in C, F, and I (*Grn*-/- in white, *Grn*+/+ in black) as mean ± SEM. Statistics denoted as $p<0.001$, ***.

Table 1

Time lines for behavioral testing of two cohorts of *Grn*-/- and *Grn*+/+ mice